

# Time-resolved detection enables standard two-photon fluorescence microscopy for *in vivo* label-free imaging of microvasculature in tissue

Dong Li,<sup>1,†</sup> Wei Zheng,<sup>1,†</sup> Wei Zhang,<sup>1</sup> Seng Khoon Teh,<sup>1</sup> Yan Zeng,<sup>1</sup> Yi Luo,<sup>2</sup> and Jianan Y. Qu<sup>1,\*</sup>

<sup>1</sup>Biomedical Engineering Program, Department of Electronic and Computer Engineering, Hong Kong University of Science and Technology, Hong Kong, China

<sup>2</sup>Bio\_X Division, Hefei National Laboratory for Physical Science at the Microscale, University of Science and Technology of China, Hefei, Anhui 230026, China

\*Corresponding author: eequ@ust.hk

Received April 4, 2011; revised June 9, 2011; accepted June 9, 2011;  
posted June 14, 2011 (Doc. ID 145373); published July 12, 2011

We conducted a systematic study on two-photon excited fluorescence (TPEF) of hemoglobin using the near transform-limited and Gaussian-shaped femtosecond pulse sources. We found that the two-photon action cross section of hemoglobin drops over 2 orders of magnitude in the wavelength range from 550 to 800 nm, while the spectral and temporal characteristics of hemoglobin TPEF are insensitive to the change of excitation wavelength. In particular, our new findings showed that the hemoglobin fluorescence could be excited with sufficient efficiency using a conventional Ti:sapphire laser tuned at the wavelength close to 700 nm. With the employment of a time-resolved detection method, we demonstrated that the TPEF signals of hemoglobin excited by a Ti:sapphire laser could be clearly differentiated from other nonlinear signals presented within the living biological tissues, indicating that a standard TPEF microscope can become a routine tool for *in vivo* label-free microangiography imaging. © 2011 Optical Society of America

OCIS codes: 180.4315, 170.1470, 180.6900, 170.6920, 170.3880.

Two-photon excited fluorescence (TPEF) microscopy is an indispensable tool for life science research and medical diagnosis [1]. Particularly, the TPEF signals of endogenous fluorescence molecules, such as reduced nicotinamide adenine dinucleotide (NADH), tryptophan, flavin adenine dinucleotide, keratin, collagen, and elastin provide rich morphological and biochemical information that is imperative toward label-free imaging of living biological systems and noninvasive diagnosis of diseases [2–5]. Very recently, we discovered that hemoglobin emitted strong Soret-band TPEF signals with unique spectral and temporal characteristics [6]. Additionally, we demonstrated that with 600 nm excitation, that hemoglobin can be used as an endogenous fluorescence contrast agent for TPEF imaging of microvasculature structures *in vivo* [7]. However, the visible ultrafast excitation source could only be obtained from an optical parametric oscillator (OPO) or a photonic crystal fiber (PCF) pumped by a Ti:sapphire femtosecond laser, which makes the excitation source more complicated and hinders the applications of hemoglobin as a fluorescence contrast agent for TPEF microscopy. On the other hand, the commercial Ti:sapphire femtosecond laser is the most commonly used excitation source for nonlinear optical imaging. Therefore, it is of a significant scientific value to investigate the use of the conventional Ti:sapphire laser as an excitation source coupled with efficient label-free contrast mechanism for *in vivo* TPEF imaging microvasculatures from the heterogeneous tissues. In this work, we conduct a systematic study of TPEF properties of hemoglobin as a function of excitation wavelength. Based on the unique temporal characteristics of hemoglobin TPEF signals, we demonstrate *in vivo* label-free imaging of microvasculature in tissue using a conventional femtosecond Ti:sapphire laser as the excitation source.

The two-photon action cross section of a fluorophore,  $\eta(\lambda_{\text{ex}})$ , can be calculated as follows [6,8]:

$$\eta(\lambda_{\text{ex}}) = \frac{\varepsilon I_f \tau_p \lambda_{\text{ex}}^2}{P_{\text{ave}}^2}, \quad (1)$$

where  $\varepsilon$ ,  $I_f$ ,  $\tau_p$ , and  $P_{\text{ave}}$  are the proportional constant, measured fluorescence intensity, excitation pulse duration, and average excitation power, respectively. The precise measurements of  $I_f$ ,  $\tau_p$ , and  $P_{\text{ave}}$  are critical to the accurate computation of  $\eta(\lambda_{\text{ex}})$ . As emphasized in our previous study, the hemoglobin fluorescence was not accurately characterized because a broadband supercontinuum light of irregular spectral distribution was used as the short-wavelength excitation source [6]. Its pulse duration measured by an autocorrelator cannot be directly compared with a Gaussian-shaped Ti:sapphire femtosecond laser covering the excitation wavelength over 700 nm. In this study, the previously employed excitation source of supercontinuum emission from a PCF was replaced by the femtosecond pulse sources with Gaussian spectral distribution to ensure accurate measurement of excitation pulse duration at different wavelengths. Specifically, the near-infrared excitation light from 680 to 1080 nm was provided by a Ti:sapphire femtosecond laser (Chameleon Ultra II, Coherent, Inc.), and the visible femtosecond pulses from 550 to 650 nm were produced by the frequency doubling of output light of a Ti:sapphire laser pumped OPO (Chameleon OPO, Coherent, Inc.). The dispersion introduced by the optics of a home-built TPEF microscope system was compensated by a prism-based compressor. This permitted the near-transform-limited pulses at the focal point of the objective (UAPO40XW3/340, 1.15NA, Olympus). At each excitation wavelength, the pulse duration  $\tau_p$  was measured by an autocorrelator (Pulsecheck-50, APE GmbH, Germany). And the  $P_{\text{ave}}$  was measured by a power meter (Model 2832-C, Newport).

Similarly to the previous study, the detection system was a multichannel time-correlated single photon counting (TCSPC) module (PML-16-0-C and SPC-150, Becker & Hickl GmbH) to record the time-resolved fluorescence signals in 16 consecutive bands from 300 to 500 nm [6,7]. In addition,  $I_f$  was represented by the summation of the acquired photon counts from 400 to 475 nm where the hemoglobin fluorescence concentrate.

The normalized relative two-photon action cross section of oxyhemoglobin and deoxyhemoglobin as functions of wavelengths are shown in Fig. 1(a). The procedures of extracting hemoglobin from fresh blood and preparing the oxyhemoglobin and deoxyhemoglobin were the same as our previous study [6]. As can be seen, though the two-photon action cross section of the two hemoglobin types are very similar and drop over 2 orders from 550 to 800 nm, the difference between excitation at 600 and 700 nm is only about a factor of 9, which is substantially smaller than that measured with a broadband supercontinuum as the short excitation wavelength [6]. This new finding indicates that a source of wavelength in 700–750 nm, typically covered by a Ti:sapphire femto-second laser, still produces sufficient excitation efficiency for label-free microvasculature imaging.

Next, we investigated the spectral and temporal characteristics of hemoglobin TPEF signal. Since the spectrum and lifetime of oxyhemoglobin and deoxyhemoglobin are similar, only the spectra of oxyhemoglobin are exemplified in Fig. 1(b). It is evident that hemoglobin fluorescence presents a fixed spectral peak around 440 nm at all excitation wavelengths used in this study except at 625 nm. The spectrum excited at 625 nm shows a slight broadening to short wavelength side due to unknown reason(s). In terms of temporal characteristics, both oxyhemoglobin and deoxyhemoglobin fluorescence present extremely short lifetime because the fluorescence time-decay curves are identical to the TCSPC instrument response,  $\sim 230$  ps, at all excitation wavelengths (data not shown). Based on these unique TPEF characteristics of hemoglobin, we explored *in vivo* imaging of microvasculature in tissue using a Ti:sapphire laser as the excitation source.

The hamster cheek pouch model was used for *in vivo* TPEF imaging. The procedures of anesthetizing the hamster were the same as our previous studies [4,7]. The sampling area of an image was  $100\ \mu\text{m} \times 100\ \mu\text{m}$  ( $128 \times 128$  pixels) and the acquisition time was set to 8 s for each optical sectioning depth. In hamster cheek pouches most of microvasculatures are located in the connective tissue

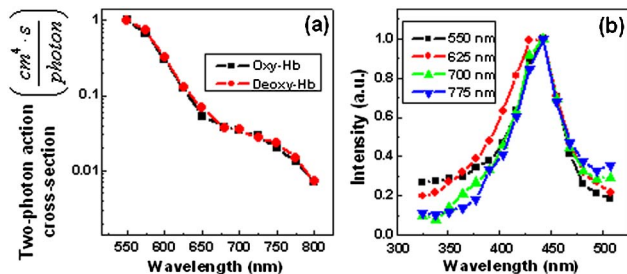


Fig. 1. (Color online) TPEF properties of hemoglobin. (a) Normalized excitation efficiency of oxyhemoglobin and deoxyhemoglobin from 550 to 800 nm; (b) TPEF spectrums of oxyhemoglobin at different excitation wavelengths.

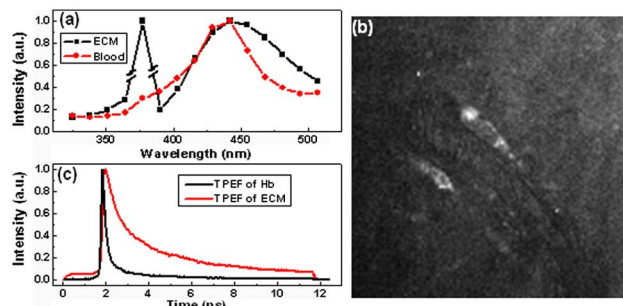


Fig. 2. (Color online) (a) Typical TPEF spectra of hemoglobin and connective tissue excited at 750 nm (the intensity of SHG signal in channel 5 was divided by a factor of 300 for clear display of spectral shape); (b) TPEF intensity image acquired from connective tissue layer of hamster oral check pouch; (c) time-decay curves of hemoglobin and connective tissue.

under epithelial layer. To investigate the contrast mechanism of differentiating a microvascular vessel from its surrounding tissue using the TPEF signals excited by a Ti:sapphire laser, we compared the fluorescence characteristics of hemoglobin with the connective tissue. Representative results are shown in Fig. 2(a). The TPEF spectra of hemoglobin overlay considerably with connective tissue signals that are mainly lying in 400 to 500 nm, and dominated by the TPEF signals of extracellular matrix (ECM) proteins, such as collagen and elastin, and the fibroblasts that serve to secrete ECM proteins [9]. To form a TPEF intensity image of connective tissue layer, we integrated the signals from 400 to 500 nm and excluded the strong second harmonic generation (SHG) signals from collagen. As can be seen in Fig. 2(b), the bright features in the middle of the image are the fibroblasts conveyed by the NADH fluorescence. The intensity image does not reveal any obvious microvasculature structures, indicating that the excitation efficiencies of TPEF signals from the hemoglobin in blood and the surrounding connective tissue are comparable. However, in time domain, the hemoglobin fluorescence presents extremely short lifetime, as shown in Fig. 2(c), while the average fluorescence of connective tissue is about 1.6 ns, much longer than hemoglobin. With time-resolved detection capability, the difference in fluorescence decay can be used to differentiate hemoglobin signals from connective tissue.

We reported a simple temporal analysis method to characterize the fluorescence decay [7]. The fundamental principle of the method is accurate calculation of the ratio of TPEF counts recorded in the first 300 ps time window over the counts recorded afterward for every image pixel. An image pixel with high ratio value can be identified as the hemoglobin TPEF signal and a pixel of low ratio value is corresponding to the slowly decaying TPEF signal of surrounding tissue. Therefore, the microvasculature can outstand in a gray scale ratio image due to the significant difference in the ratio between the hemoglobin in blood vessels and the surrounding connective tissue. The representative gray scale ratio images acquired at different excitation wavelengths and powers are shown in Fig. 3. The measurement site was the same as the intensity image shown in Fig. 2(b). As shown in the figure, even the excitation efficiency in the wavelength range of a Ti:sapphire laser is significantly lower than

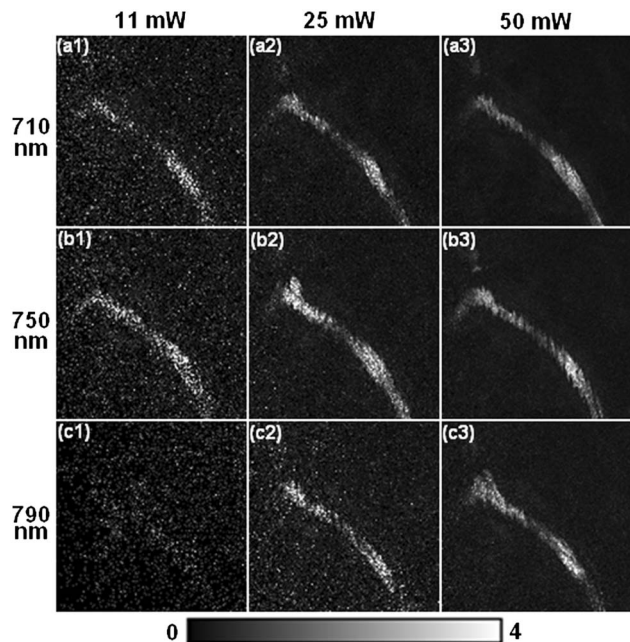


Fig. 3. Representative gray scale temporal intensity ratio images at different excitation wavelengths and powers: (a1)–(a3) excited at 710 nm; (b1)–(b3) excited at 750 nm; (c1)–(c3) excited at 790 nm. The excitation powers of left, middle, and right column images are 11, 25, and 50 mW, respectively. The sampling site locates 60  $\mu\text{m}$  below the top surface of hamster oral tissue.

the visible region; the microvasculature structures still can be identified clearly as long as enough photons for every image pixel are accumulated for accurate calculation of the ratio. It is indeed noticed that under a compromised signal-to-noise ratio (SNR) condition notable salt-and-pepper noises appear in the ratio image, concealing the microvasculature, as shown in the images excited at long wavelengths or low powers. In the poor SNR situation, if the pixels of surrounding tissue collected no or only few photons in the decay time latter than 300 ps, they would present very high ratio that contributed to the salt-and-pepper noise. Moreover, the photomultiplier tube (PMT) dark counts, which randomly appear in the fluorescence time-decay curve, can also significantly distort the ratio in a poor SNR situation. In general, longer excitation wavelengths require higher excitation power to accumulate enough photons for accurate ratio calculation due to the lower excitation efficiency. Overall, the results provide solid evidence that a standard TPEF microscope equipped with a commercial Ti:sapphire femtosecond laser and a time-resolved fluorescence detection system is able to perform *in vivo* label-free imaging of microvasculature at biocompatible excitation power levels and reasonable acquisition time.

The depth-resolved TPEF images of the hamster oral tissue and the reconstructed 3D image of the microvascular network are shown in Fig. 4 to further demonstrate the *in vivo* TPEF imaging of microvasculature using a standard Ti:sapphire femtosecond source. The detailed results can be found in Media 1 and Media 2, respectively. As can be seen in Fig. 4(a), in addition to the SHG signal of collagen and the TPEF signals of NADH in cells and proteins in ECM, the TPEF signals of hemoglobin were

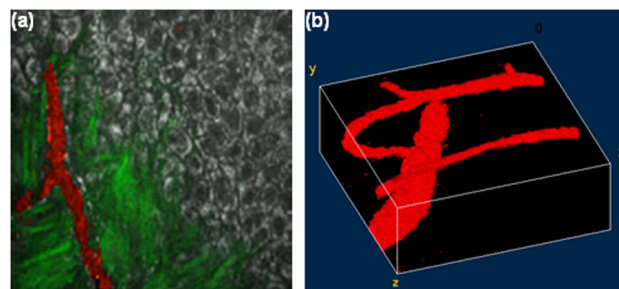


Fig. 4. (Color online) Representative TPEF images of the hamster oral tissue *in vivo* with 25 mW excitation at 710 nm wavelength. (a) Typical TPEF image at the junction layer between epithelium and connective tissue. SHG signals and TPEF of hemoglobin are colored in green and red, respectively. Other slowly decaying TPEF signals are in gray scale. (Detailed depth-resolved TPEF images starting from stratum basal layer are shown in Media 1.) (b) The 3D image of the microvascular networks reconstructed from the depth-resolved TPEF images (see detail in Media 2).

identified by establishing an optimal threshold in the histogram of ratio image. All these nonlinear optical signals facilitated us to simultaneously label-free image the cell morphology, the distribution of collagen fibers, and microvasculature. Finally, the 3D structure of the microvascular network was reconstructed using the depth-resolved TPEF images of hemoglobin fluorescence. As can be seen from Fig. 3(b) and Media 2, the microvasculature with complex 3D distribution could be clearly elucidated based on depth-resolved TPEF imaging with a Ti:sapphire laser as the excitation source.

In conclusion, we demonstrate that a standard TPEF microscope coupled with a time-resolved detection system can become a routine tool for *in vivo* label-free microvasculature imaging. Moreover, the fluorescent properties of hemoglobin were accurately characterized. The TCSPC-based time-resolved detection is a mature technique and the cost is negligible compared with the two-photon microscopy system. The overall detection sensitivity can be significantly improved by replacing the low efficient spectra-resolved detection system with a cooled single PMT. Consequently, the excitation power will be reduced to prevent any possible phototoxicity.

<sup>†</sup>These authors contributed equally to this work.

## References

1. B. R. Masters and P. T. C. So, *Handbook of Biomedical Nonlinear Optics* (Oxford, 2008).
2. W. R. Zipfel, R. M. Williams, R. Christiet, A. Y. Nikitin, B. T. Hyman, and W. W. Webb, *Proc. Natl. Acad. Sci. USA* **100**, 7075 (2003).
3. D. Li, W. Zheng, and J. Y. Qu, *Opt. Lett.* **34**, 202 (2009).
4. D. Li, W. Zheng, and J. Y. Qu, *Opt. Lett.* **34**, 2853 (2009).
5. H. G. Breunig, H. Studier, and K. Konig, *Opt. Express* **18**, 7857 (2010).
6. W. Zheng, D. Li, Y. Zeng, Y. Luo, and J. Y. Qu, *Biomed. Opt. Express* **2**, 71 (2011).
7. D. Li, W. Zheng, Y. Zeng, Y. Luo, and J. Y. Qu, *Opt. Lett.* **36**, 834 (2011).
8. C. Xu and W. W. Webb, *J. Opt. Soc. Am. B* **13**, 481 (1996).
9. W. Zheng, Y. Wu, D. Li, and J. Y. Qu, *J. Biomed. Opt.* **13**, 054010 (2008).